Structure factors of charged bidispersed colloidal suspensions

1992 J. Phys.: Condens. Matter 4 3077

(http://iopscience.iop.org/0953-8984/4/12/007)

J. Phys.: Condens. Matter 4 (1992) 3077–3086. Printed in the UK

Structure factors of charged bidispersed colloidal suspensions

B D'Aguanno, R Krause, J M Méndez-Alcaraz and R Klein
Fakultät für Physik, Universität Konstanz, Postfach 5560, 7750 Konstanz, Federal Republic of Germany

Received 4 September 1991, in final form 4 November 1991

Abstract. In the present study, the effects of charge bidispersity on static structure factors of dilute charged aqueous colloidal suspensions, for compositions covering the full molar fraction range, are investigated using static light-scattering experiments and integral equation theory. The suspensions under study are made from different charged polystyrene particles with an average diameter of 100 nm. The experimentally-observed static structure factors are then compared with theoretical results obtained from the hypernetted chain approximation. The values of both charges are determined by fitting the scattering data of the two pure components and are kept constant for the mixtures. In order to fully describe the experimental data, the effects of the intrinsic polydispersity have to be taken into account. It is found that the height of the main peak of the measured static structure factor, $S^{M}(q)$, changes monotonically as a function of the composition.

1. Introduction

Polydispersity of charge and size is a natural and unavoidable characteristic of charge-stabilized colloidal suspensions. The influence of both polydispersities on the structural and scattering properties of two-component mixtures has been previously analysed by us and the results of such a study are reported in [1]. However, the quantification of the separate charge and size polydispersity effects on these properties is cumbersome [2, 3]. To understand the effects of the charge polydispersity alone, and to analyse the differences between this case and the more general case of combined charge and size polydispersity, we will investigate, in the full molar range, binary mixtures of polystyrene latex particles in which the two components have the same average diameters but different average charges. An important qualitative difference between the two kinds of polydispersed systems lies in the fact that, for charge polydispersed systems the measured scattered intensity is directly related to the mean particle distribution, without containing any information on the intraparticle structure. The same is not true for charge and size polydispersed systems. With respect to these considerations, the present work can be seen as a continuation of our previously published study [1]. The experimental investigation is made using the static light-scattering (SLS) technique. The interpretation of the experimental data is then made by solving the hypernetted chain closure (HNC) of the Ornstein–Zernike equation for both the bidispersed and polydispersed models of the mixtures.

In the bidispersed model the size distribution of the two components is given by two delta functions centred at the particle diameter whereas the charge distributions are given by two delta functions centred at the two different charge values.

0953-8984/92/123077+10$04.50

In the more realistic but complex polydispersed model, the intrinsic size polydispersity is introduced and, since the charges on the particles are linked to their sizes, the intrinsic charge polydispersity is also taken into account. The size distribution of the mixtures is given by two Schulz distributions centred at the average particle diameter and the charge distributions by two other Schulz distributions centred at the two different average charges. To fully describe all the features of the measured structure factor, $S^{M}(q)$, we have to rely on the polydispersed model.

In the next section a short summary of the scattering relations and of the HNC theory for multi-component systems is given. In section 3 we describe the experimental setup and the sample preparation. In the last section we present comparisons and discussions of experimental data with theoretical results.

2. Scattering relations and integral equation theory

In a SLS experiment, the measured scattered intensity from a sample having N particles of p different species is given by

$$I(q) = \left\langle \left| \sum_{\alpha=1}^{p} \sum_{i=1}^{N_\alpha} b_\alpha(q) e^{i\mathbf{q}\mathbf{r}_i^\alpha} \right|^2 \right\rangle . \tag{1}$$

where N_α is the number of particles of species α, r_i^α the position of the particle i of species α, $b_\alpha(q)$ the corresponding scattering amplitude, q the magnitude of the scattering wavevector q and $\langle \ldots \rangle$ the configurational average. Introducing the partial structure factors $S_{\alpha\beta}(q)$

$$S_{\alpha\beta}(q) = \frac{1}{N} \sum_{i=1}^{N_\alpha} \sum_{j=1}^{N_\beta} \langle e^{i\mathbf{q}(\mathbf{r}_i^\alpha - \mathbf{r}_j^\beta)} \rangle = x_\alpha \delta_{\alpha\beta} + n x_\alpha x_\beta \tilde{h}_{\alpha\beta}(q) \tag{2}$$

the scattering intensity per unit of volume, $I(q)$, becomes

$$I(q) = n \sum_{\alpha,\beta=1}^{p} b_\alpha(q) b_\beta(q) S_{\alpha\beta}(q) \tag{3}$$

where $x_\alpha = N_\alpha / N$ is the molar fraction of the α-particles, n the total number density of the sample and $\tilde{h}_{\alpha\beta}(q)$ the Fourier transform of the total correlation function $h_{\alpha\beta}(r)$. This relation is usually rewritten as follows

$$I(q) = n \overline{P(q)} S^{M}(q) \tag{4}$$

where the form factor $\overline{P(q)}$ is given by the following average over the particle type distribution

$$\overline{P(q)} = \sum_{\alpha=1}^{p} x_\alpha b_\alpha^2(q). \tag{5}$$

For a spherical particle of diameter σ_α and of homogeneous scattering material, the expression for the scattering amplitude $b_\alpha(q)$ is

$$b_\alpha(q) = V_\alpha(n_\alpha - n_s)\frac{3j_1(q\sigma_\alpha/2)}{q\sigma_\alpha/2} \tag{6}$$

where V_α is the volume of the particle α, n_α and n_s are the refractive indices of the particles and of the solvent, respectively, and j_1 is the first-order spherical Bessel function.

From equations (3) and (4), the measured structure factor $S^M(q)$ is given by

$$S^M(q) = \frac{1}{\overline{P(q)}} \sum_{\alpha,\beta=1}^{p} b_\alpha(q)b_\beta(q)S_{\alpha\beta}(q). \tag{7}$$

This is a completely general relation and can be used to describe all the cases in which the particles differ either in size and/or charge and/or scattering power.

Equation (7) shows that the information contained in $S^M(q)$ depends on both single-particle scattering properties and on interparticle structural properties. The case of $p = 1$ (monodispersed sample) is more simple and $S^M(q)$ coincides with the particle–particle structure factor.

From the experimental point of view, the measured structure factor, $S^M(q)$, which is the quantity of primary interest here, is extracted from the measured intensities taking the ratio

$$S^M(q) = \frac{n_0}{n}\frac{I(q)}{I_0(q)} \tag{8}$$

where $I_0(q)$ is the intensity of a dilute non-interacting sample with number density n_0

$$I_0(q) = n_0\overline{P(q)}. \tag{9}$$

In the present investigation we are interested in the case of two-component mixtures, in which the mean charge of component 1 is different from the mean charge of component 2 and the mean diameters of both components are equal. To study the mixtures, we will use two models. In the first model, the mixtures are represented by particles with exactly the same diameters, but with two possible values of their charges, and we call this ideal case the *bidisperse* mixture. For the ideal charge bidispersed mixture (7) simplifies to

$$S^M(q) = \sum_{\alpha,\beta=1}^{2} S_{\alpha\beta}(q). \tag{10}$$

This combination of partial structure factors is just equal to the number–number structure factor $S_{NN}(q)$ [3, 4], which describes the correlations of the fluctuations of the *total* number density.

In the second more realistic and complex model, the unavoidable size polydispersity of the particles is taken into account. The intrinsic size polydispersity is described by a histogrammatic version of the continuous Schulz distribution

$$f(\sigma) = \left(\frac{t+1}{\langle\sigma\rangle}\right)^{t+1}\frac{\sigma^t}{\Gamma(t+1)}\exp\left[-\frac{t+1}{\langle\sigma\rangle}\sigma\right] \qquad (t > 0) \tag{11}$$

in which the positions and the heights of the components are determined requiring the equality of higher moments of both the histogrammatic and continuous distributions (for details see [1, 2]). Here t is a measure of the width of the distribution and $\Gamma(t)$ is the Gamma function. Since there is no experimental information on the variation of the particle charge as a function of the particle size we assume that the charges on the particles scale linearly with their surfaces. The validity of this assumption will be verified *a posteriori*, after comparing the results from our model with the experimental data on the structure. The intrinsic size polydispersity determines the charge distribution of the samples. This is given by the sum of two Schulz distributions centred around the two different average charges. This situation is somewhat more complicated than in the ideal charge bidispersed system, where the charge distribution is simply the sum of two delta functions; in real suspensions the unavoidable size polydispersity leads to a certain smearing out of the delta functions. This more realistic case is referred to as the *polydispersed* mixture.

To theoretically determine $S^{M}(q)$ it is, therefore, necessary to solve the multicomponent Ornstein–Zernike (OZ) equations together with a closure relation [5]. Using the HNC closure [3], the complete set of equations to be solved is

$$h_{\alpha\beta}(r) = c_{\alpha\beta}(r) + n\sum_{\gamma=1}^{p} x_\gamma \int \mathrm{d}r'\, h_{\alpha\gamma}(r')c_{\gamma\beta}(|r-r'|) \qquad \text{(OZ)} \tag{12}$$

$$h_{\alpha\beta}(r) = -1 + \exp[-\beta u_{\alpha\beta}(r) + h_{\alpha\beta}(r) - c_{\alpha\beta}(r)] \qquad \text{(HNC)}. \tag{13}$$

For the interaction potentials, $u_{\alpha\beta}(r)$, appearing in the HNC closure we take the repulsive parts of the Derjaguin–Landau–Verwey–Overbeek (DLVO) potentials [6]

$$u_{\alpha\beta}(r) = \frac{Q_\alpha Q_\beta}{4\pi\epsilon\epsilon_0}\left(\frac{\mathrm{e}^{\kappa\sigma_\alpha/2}}{1+\kappa\sigma_\alpha/2}\right)\left(\frac{\mathrm{e}^{\kappa\sigma_\beta/2}}{1+\kappa\sigma_\beta/2}\right)\frac{\mathrm{e}^{-\kappa r}}{r} \qquad r > \sigma_{\alpha\beta} = (\sigma_\alpha+\sigma_\beta)/2$$
$$= \infty \qquad r < \sigma_{\alpha\beta}. \tag{14}$$

Here Q_α is an effective charge on particles of species α. The effective charge is introduced in order to write the interaction potential in the DLVO form of the previous equation and, strictly speaking, it does not have an obvious physical meaning [7]. The inverse Debye–Hückel screening length κ is defined as

$$\kappa = \left(\frac{1}{\epsilon\epsilon_0 k_B T}\sum_\alpha n_\alpha q_\alpha^2\right)^{1/2} \tag{15}$$

in which the sum is over the counterions and added ions present in the sample and q_α and n_α are their charge and partial number density, respectively.

When the system of (12) and (13) is solved with respect to $h_{\alpha\beta}(r)$ and $c_{\alpha\beta}(r)$, the partial structure factors $S_{\alpha\beta}(q)$ appearing in (7) and (10) are obtained from (2).

3. Experimental details

A focused 3 W argon laser beam, with wavelength $\lambda_0 = 488$ nm, was directed into a temperature-stabilized ($T = 21 \pm 1\,^{\circ}\mathrm{C}$) cylindrical sample cell of 10 mm outer

diameter and containing approximately 2 ml of colloidal dispersion. The photon counts of the photomultiplier were processed for further data evaluation by a digital correlator (ALV-3000, FRG) linked to a computer. Intensity data were corrected for the dark rate of the photomultiplier and for the angular dependence of the scattering volume. The magnitude of the scattering vector, $q = (4\pi n_s/\lambda_0)\sin(\Theta/2)$, ranges from 3 to 33×10^{-3} nm^{-1}. Here, Θ is the scattering angle and $n_s = 1.33$ is the solvent refractive index. All experimental results reported in this work were obtained with an angle resolution of 1° steps. To characterize the peak height of the measured intensity well, additional measurements in the region of the first peak were performed with an angle resolution of 0.5° steps.

The samples were diluted from highly concentrated polystyrene solutions (DOW Chemical) using deionized water. The five charge bidispersed samples were composed out of two well characterized pure monodispersed batches of polystyrene spheres with the average diameter $\sigma = 100$ nm and with two different surface valencies, at five different partial volume fractions $\Phi_\alpha = (\pi n_\alpha \sigma_\alpha^3)/6$, $(\alpha = 1, 2)$. The difference in the two surface valencies arises from the partial replacements of sulphate surface groups by carbonate groups, which have different dissociation constant. The composition of the mixtures were also characterized by the molar fractions $x_1 = N_1/(N_1 + N_2)$ of species 1, where N_1 is the particle number of species 1. In order to minimize the ionic strength of the suspensions, a cleaned mixed-bed ion exchange resin was added to the samples, removing all small ions other than H^+ and OH^-. No investigations with added salt were made, since we were interested in strongly coupled systems.

To characterize the particles, dynamic light scattering (DLS) experiments on very dilute samples of each of the two pure components were performed and we obtained the same average diameter for both batches. The fact that the dynamic correlation functions exhibit a finite second cumulant, Γ_2, shows that the so-called pure components are, to some extent, polydispersed. From the cumulant analysis [8, 9] we determined the standard deviation s_σ of the particle size using the relation $s_\sigma = \Gamma_2/\Gamma_1^2$, where Γ_1 is the first cumulant. It is with this qualification that we use the word 'monodisperse' when speaking about the samples with $x_1 = 0$ and $x_1 = 1$. For the standard deviation of the particle size, the value $s_\sigma = 0.12 \pm 0.03$ was obtained. The DLS experiments were performed in the homodyne mode.

A summary of the parameters characterizing the systems used in this study is given in tables 1 and 2.

Table 1. Parameters characterizing the macro-ions of the pure components, using the monodisperse as well as the polydispersed model.

Species	σ(nm)	$Q_{\text{poly}}^{\text{HNC}}(e)$	$Q_{\text{mono}}^{\text{RMSA}}(e)$	$Q_{\text{mono}}^{\text{HNC}}(e)$
1	100	700	520	513
2	100	480	400	390

4. Results

In this section we present the comparisons between integral equation theories and experimental SLS data.

Table 2. *Volume fractions of all seven samples under study, as well as the molar fractions of species 1, using the intrinsic polydispersity, $s_\sigma = 0.1$, within the HNC closure.*

Sample	$\Phi_1^{exp}(\times 10^{-4})$	$\Phi_2^{exp}(\times 10^{-4})$	$\Phi_1^{fit}(\text{poly})(\times 10^{-4})$	$\Phi_2^{fit}(\text{poly})(\times 10^{-4})$	x_1
1	5	0	4.85	0	1
2	0	5	0	3.70	0
3	0.5	4.5	0.490	3.95	0.11
4	1.5	3.5	1.59	3.32	0.324
5	2.5	2.5	2.52	1.95	0.563
6	3.5	1.5	3.53	1.18	0.75
7	4.5	0.5	4.35	0.380	0.92

The SLS experiments have been performed on the seven samples whose experimentally determined parameters are listed in table 2 (columns 2 and 3). The diameters of the two species are the same and have a value of $\sigma_1 = \sigma_2 = 100$ nm.

Figure 1 shows SLS data and the HNC(poly) results from the intrinsic polydispersity model introduced in the second section. To obtain these results we proceed in the following way. First the concentrations and the charges of species 1 and 2 are determined by fitting the peak position and the peak height of $S^M(q)$ of the two pure samples (samples 1 and 2). Subsequently, keeping the determined charges fixed, the results of the intermediate samples (samples 3 to 7) are obtained by adjusting the concentrations of both components. The adjusted values of the concentrations are well inside the experimental error of the method used for the determination of the concentration. A summary of the particle and sample parameters used in these calculations is given in table 1 (columns 2 and 3) and table 2 (columns 4 and 5). As it is evident from the figure, the intrinsic polydispersed model and the fitting procedure described earlier generate a quantitative agreement with the experimental data.

To illustrate the influence of the intrinsic polydispersity of the two 'pure' components on the results for the mixtures, we show in figure 2, which refers to sample 5, the SLS data together with results from the polydispersed model, HNC(poly), and a model treating the 'pure' components as truly monodispersed; the latter results are referred to as HNC(bidis). As in the case of charge and size polydispersed systems (see [1]), the inclusion of the intrinsic polydispersity of each component results in a better agreement with the experimental data.

Although the differences between the HNC(poly) and HNC(bidis) results seem quite small on the scale of the figure, we note that the value of $S^M(q = 0)$ from the HNC(poly) is approximately three times larger than the corresponding value from the HNC(bidis) (for a better view see figure 5). This drastic variation is due to the fact that when the intrinsic size and charge polydispersity of each component is taken into account, $S^M(q)$ has to be evaluated using (7), which depends on the form amplitudes $b_\alpha(q)$. The latter reflects the particle size distribution. If the size polydispersity is neglected, so that only the charge bidispersity is taken into account, $S^M(q)$ is given by (10). Using a slightly different language [10], we can say that in the charge bidispersed case there is no incoherent contribution to the scattering, whereas in the intrinsic size and charge polydispersed case this contribution is different from zero.

Now we discuss several features of the measured structure factors as a function of the molar fraction x_1. Figure 3 shows the peak values, S^M_{max}, of $S^M(q)$ ranging from the pure sample 2 to the pure sample 1. The good agreement between the SLS data and the theoretical results reflects the correctness of the assumption of constant

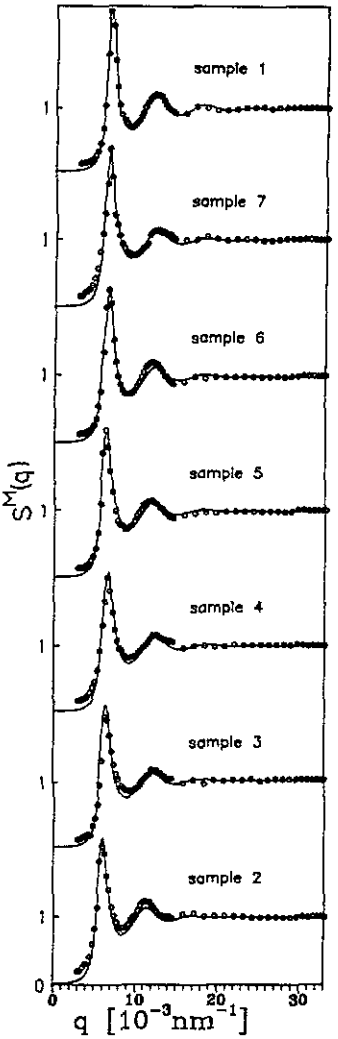

Figure 1. Structure factors, $S^M(q)$, of the seven investigated samples: experimental data, dots; HNC(poly)-fits, full curve. The system parameters are listed in table 1 and 2.

particle charges as a function of the molar fraction. In figure 3 the SLS data are also compared with the rescaled mean spherical approximation (RMSA) [1, 11] results. From the good agreement which is observed in this case, it can be concluded that the previous assumption about the particle charges applies to the class of systems investigated here.

The monotonic increase of the peak values arises from the increase of the mean charge, $\langle Q \rangle$, of the particles (see figure 4). This is more evident from the charge bidispersed model in which $S^M(q)$, as given by (10), coincides with the Bhatia–Thornton structure factor $S_{NN}(q)$: it is a well known fact that the peak of $S_{NN}(q)$ increases with increasing particle interaction strength [3, 12]. For size and charge bidispersed systems [1], a non-monotonic behaviour of S^M_{max} was found but in that case, and in contrast to the present case, the standard deviation of the particle size changed as a function of the molar fraction.

The variation of the mean charge of the particles, $\langle Q \rangle$, is shown in figure 4

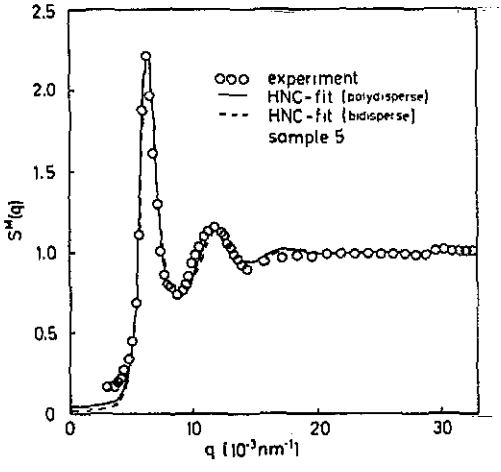

Figure 2. Comparison between the experimental $S^M(q)$ data (dots), the HNC(poly) results (full curve) and the HNC(bidis) results (broken curve) of sample 5.

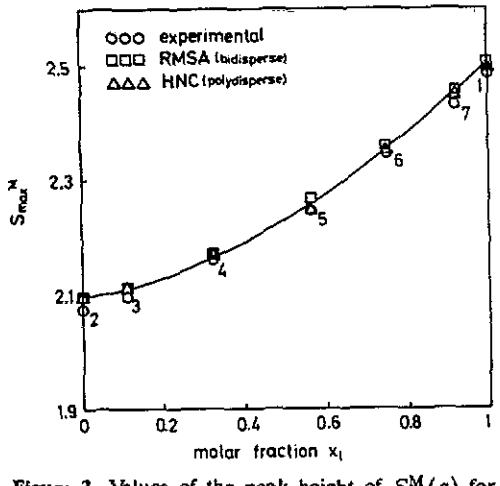

Figure 3. Values of the peak height of $S^M(q)$ for all studied samples as a function of the molar fraction x_1 of component 1.

together with the standard deviation of the charge, $s_Q = (\langle Q^2\rangle - \langle Q\rangle^2)^{1/2}/\langle Q\rangle$. This quantity has a large influence on the behaviour of $S^M(q)$ at $q = 0$. Although $S^M(q = 0)$ cannot be directly measured, it is worthwhile to show the theoretically determined $S^M(q = 0)$ as a function of x_1. The HNC results of $S^M(q = 0)$, from both the bidispersed and the intrinsically polydispersed model, are presented in figure 5. The charge bidispersed model generates values of $S^M(q = 0)$ ($\equiv S_{NN}(0)$) that have a maximum which corresponds to the maximum of the charge bidispersity s_Q. For a two-component system the Bhatia–Thornton structure factors are linked to the isothermal compressibility via the relation [3]

$$S_{NN}(0) = nk_BT\kappa_T + \frac{S^2_{CN}(0)}{S_{CC}(0)} \qquad (16)$$

where $S_{CN}(0)$ and $S_{CC}(0)$ are the charge-number and the charge–charge structure

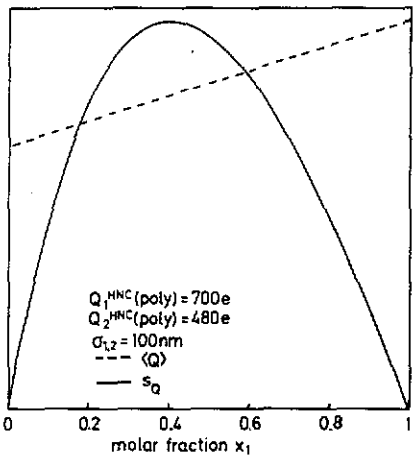

Figure 4. Standard deviation s_Q of the charge bidispersity (full curve) and mean value of the effective particle charge (broken line) as a function of the molar fraction x_1.

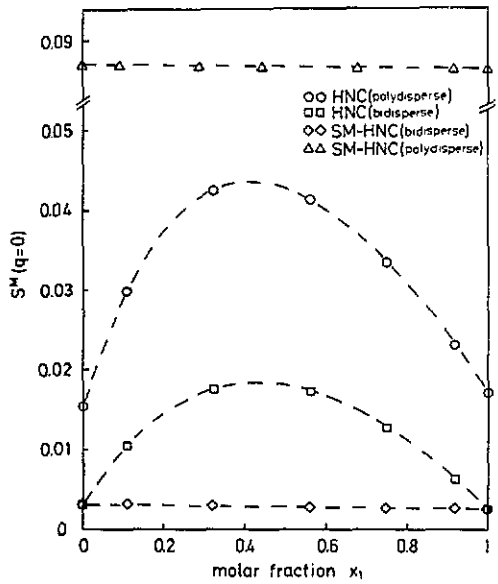

Figure 5. Values of $S^M(q = 0)$ as a function of the molar fraction x_1. The polynomial fits (broken curves) are drawn only to guide eye.

factors at $q = 0$, respectively. In going from $x_1 = 0$ to $x_1 = 1$ the values of $nk_BT\kappa_T$ are approximately constant (diamond symbols in figure 5) and then the maximum of $S_{NN}(0)$ follows from a faster increase of the charge-number fluctuations as compared to the charge–charge fluctuations when s_Q is increased, as already shown [3]. The introduction of the intrinsic polydispersity of the two pure components appreciably changes the values of $S^M(q = 0)$ to higher values, as is also shown in figure 5. Already at both ends of the molar fraction scale, $S^M(q = 0)$ is no longer equal to the normalized isothermal compressibility of the systems [2], $\chi = nk_BT\kappa_T$; for all values of x_1 there are contributions to $S^M(q = 0)$ arising from the form amplitudes in (7), which do not appear in (10) and (16). These last two equations apply to the

ideal charge bidispersed case only. The ratio of $S^{M}(0)$ (poly) and $S^{M}(0)$ (bidis) is practically a constant because the size polydispersity s_σ is independent of x_1.

Another method which is often used in the literature to fit the experimental data is the substitutional method [13, 14], SM, in which, essentially, the interaction potentials between the different species are replaced by an averaged potential over the molar fractions. The substitutional method is an acceptable approximation for systems showing size polydispersity only [3], but it fails for cases in which charge polydispersity is present. For the present charge bidispersed cases, the SM gives values of $S^{M}(q = 0)$ which, on the scale of figure 5, are indistinguishable from the values of the normalized isothermal compressibility (diamond symbols). The introduction of the intrinsic polydispersity does not improve the output of the SM, and these results (triangular symbols in figure 5) show an incorrect linear behaviour as a function of x_1.

Acknowledgments

We thank Dr G Nägele for the supply of the extended RMSA program and Dr T Palberg for the supply of the pure samples of latex particles. This work has been supported by the Deutsche Forschungsgemeinschaft (SFB306). One of us (JMM-A) acknowledges a fellowship from the Deutsche Akademische Austauschdienst (DAAD).

References

[1] Krause R, D'Aguanno B, Méndez-Alcaraz J M, Nägele G, Klein R and Weber R 1991 *J. Phys.: Condens. Matter* **3** 4459
[2] D'Aguanno B and Klein R 1991 *J. Chem. Soc. Faraday Trans.* **87** 379
[3] Méndez-Alcaraz J M, D'Aguanno B and Klein R 1991 *Physica* A **178** 421
[4] Bhatia A B and Thornton D E 1970 *Phys. Rev.* B **2** 3004
[5] Hansen J P and McDonald I R 1986 *Theory of Simple Liquids* (London: Academic)
[6] Verwey E J W and Overbeek J T G 1948 *Theory of the Stability of Lyophobic Colloids* (Amsterdam: Elsevier)
[7] Belloni L 1986 *J. Chem. Phys.* **85** 519
[8] Ackerson B J 1976 *J. Chem. Phys.* **64** 242
[9] Ackerson B J 1978 *J. Chem. Phys.* **69** 684
[10] Pusey P N, Fijnaut H M and Vrij A 1982 *J. Chem. Phys.* **77** 4270
[11] Ruiz-Estrada H, Medina-Noyola M and Nägele G 1990 *Physica* A **168** 919
[12] March N H and Tosi M P 1984 *Coulomb Liquids* (London: Academic)
[13] Faber J E and Ziman J M 1965 *Phil. Mag.* **11** 153
[14] Tata B V R, Kesavamoorthy R and Sood A K 1987 *Mol. Phys.* **61** 943